ELSEVIER

Journal of Power Sources 53 (1995) 163–173

JOURNAL OF POWER SOURCES

In situ redox conductivity, XPS and impedance spectroscopy studies of passive layers formed on lead–tin alloys

P. Simon, N. Bui, N. Pebere, F. Dabosi

Ecole Nationale Supérieure de Chimie de Toulouse, Equipe de Métallurgie Physique, Laboratoire des Matériaux URA-CNRS 445, 118 route de Narbonne, 31077 Toulouse, France

Received 3 August 1994; accepted 16 August 1994

Abstract

Lead–tin alloys (up to 2.5 wt.% Sn) have been passivated in deaerated sodium tetraborate solution (pH = 9.1). The electronic conductivity of the passive films, evaluated by the exchange current density of a redox system, increases sharply when the alloying tin content is increased from 0.8 to 1.5 wt.% Sn. X-ray photoelectron spectroscopy (XPS) signals for lead, tin and oxygen in the passive films are shifted to higher binding energies when the passive films are non-conducting. The conductivity of the passive films is related to a marked enrichment of tin oxide. An impedance spectroscopy study has shown that the polarization resistance of the passivated electrodes increases in tetraborate solution when the alloying tin content is increased. The same alloys are passivated in sulfuric acid solutions and develop an oxide film under the sulfate layer. Results show that without tin, the oxide layer behaves as a semiconductor. With tin, the composite lead–tin oxide is electronically conducting and non-ionically conducting in pH = 9.1 solution, but in sulfuric acid tin oxide is unstable and increases the ionic conductivity of the passive layers.

Keywords: Lead–tin alloys; X-ray photoelectron spectroscopy; Impedance spectroscopy; Redox conductivity

1. Introduction

With the modern tendency for the lead/acid battery industry to produce maintenance-free and valve-regulated units, low-antimony or antimony-free lead alloys have been used in order to minimize loss of water from the electrolyte. These new alloys have, however, the disadvantage of developing a passive layer that impedes electronic conduction through the grid/active-material interface. This results in loss of cycling capacity, low performance of the positive electrode, and low charge acceptance for deep-discharge batteries [1,2]. The passive layer has been identified as tetragonal-PbO (or α-PbO) that is formed under a lead sulfate layer [3–6] in a region where the pH is increased to a value of 9.3 by selective diffusion of OH^- ions. To alleviate the problem of grid passivation, the addition of tin to lead has been found [7–9] to be effective. The mechanism of the action of tin on the properties of the PbO passive layer, however, has still to be elucidated. The key question is: how much tin has to be added to lead in order to reach the optimal electrochemical properties and to induce a marked change in the electrical conduction of the PbO layer? To answer this question, tin-modified PbO layers have to be analyzed to gain a better insight into the nature, the chemical composition and the thickness of the passive films.

To understand more about the influence of tin, in situ measurements of the conductivity of the passive layers have been carried out in the work reported here by analyzing the kinetics of redox reactions on the passive electrode, and by using electrochemical impedance spectroscopy. Furthermore, surface analysis, in particular X-ray photoelectron spectroscopy, has been performed.

2. Experimental

Lead–tin alloys were prepared by melting weighed mixtures of pure lead (99.999 wt.%) and pure tin (99.99 wt.%) in an alumina crucible. The tin content of the alloys was 0.5, 0.8, 1, 1.3, 1.5 and 2.5 wt.%.

Control of the passive film growth was achieved by the classical polarization technique. All the potentials quoted in this study are reported with respect to an

SSDI 0378-7753(94)01986-6

Hg/Hg_2SO_4 saturated K_2SO_4 reference electrode (SSE). Electronic conduction of the passive layers was evaluated by measuring the polarization currents of the ferro/ferricyanide couple (0.025 M) which was added to the 0.1 M $Na_2B_4O_7$ solution (pH = 9.1) in the passive potential range of the alloy electrode (0 to +400 mV). The electrochemical impedance apparatus was composed of a Solartron Schlumberger 1250 frequency response analyser and Solartron electrochemical interface. The data were processed by a Hewlett Packard 9000 computer.

Surface analysis of the passive layers was carried out with a VGA Scientific MKII (ESCALAB) apparatus, using an Mg Kα X-ray source ($h\nu$ = 1253.6 eV). The X-ray power was 300 W.

3. Results and discussion

3.1. Electrochemical polarization of lead–tin alloys in 0.1 M $Na_2B_4O_7$

Fig. 1 shows cyclic voltammograms for pure lead and lead–tin alloys in 0.1 M $Na_2B_4O_7$ solution. For pure lead, three anodic peaks – denoted as (A), (B) and (C) – begin to appear at about −1000, −920 and +350 mV, respectively. In addition, two small cathodic peaks, D1 and D2, begin at about 200 and −125 mV, respectively, and a large cathodic peak (E) at about −920 mV.

Peak (A) is associated with the formation of $Pb(OH)_2$ [10]. Peak (B) is related to the oxidation of Pb to PbO, the equilibrium potential of which is −922 mV at pH = 9.1 [11]. This reaction occurs with a release of protons that lower the pH at the electrode surface and increase the dissolution of Pb as Pb^{2+}. When the PbO layer is sufficiently thick, the oxidation rate decreases, due to the insulating properties of PbO.

The polarization curve of a pure tin electrode in 0.1 M $Na_2B_4O_7$ solution can be seen in Fig. 2. In a pH = 9.1 solution, the only thermodynamically stable oxide that can be formed on tin is SnO_2 [11]. The equilibrium potential of the Sn/SnO_2 couple is −1285 mV. From Fig. 2, it appears that the oxidation of pure tin in 0.1 M $Na_2B_4O_7$ solution takes place at −1270 mV. This value is in good agreement with the equilibrium potential of the Sn/SnO_2 couple. After the SnO_2 formation, the current increases very slightly. At the end of the anodic scan, the increase in current indicates the beginning of oxygen evolution. On the reverse scan, only one cathodic peak is visible, beginning at −1280 mV. This corresponds to the start of the reduction of SnO_2 to metallic tin at pH = 9.1 [11].

In Fig. 1, it can be seen that the intensity of peak (A), which was attributed to the formation of $Pb(OH)_2$, decreases as the tin content in the alloys increases. For 1.5 and 2.5 wt.% Sn, this peak is greatly reduced. The same observation can be made for peak (B) that is related to the formation of PbO. The higher the tin content in the alloys, the less the amount of PbO that is formed. Thus, it can be concluded that tin inhibits the oxidation of Pb to Pb^{2+}. The intensity of peak (C) decreases with tin content. For the 2.5 wt.% Sn alloy, peak (C) is obviously composed of two peaks C_1 and C_2. C_1 appears to be present on both pure lead and lead–tin alloys. With pure lead, it is possible to see a shoulder on peak (C), marked with an arrow in Fig. 1. As the global intensity of peak (C) decreases with

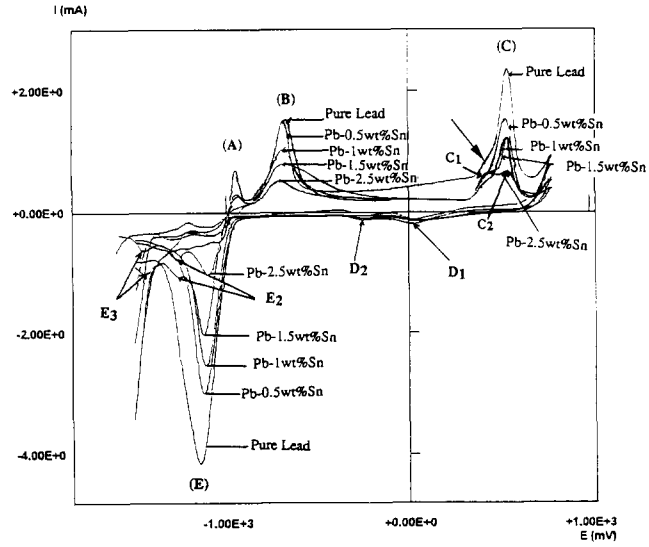

Fig. 1. Cyclic voltammograms for pure lead and different lead–tin alloys in 0.1 M $Na_2B_4O_7$. Scan rate: 10 mV s^{-1}.

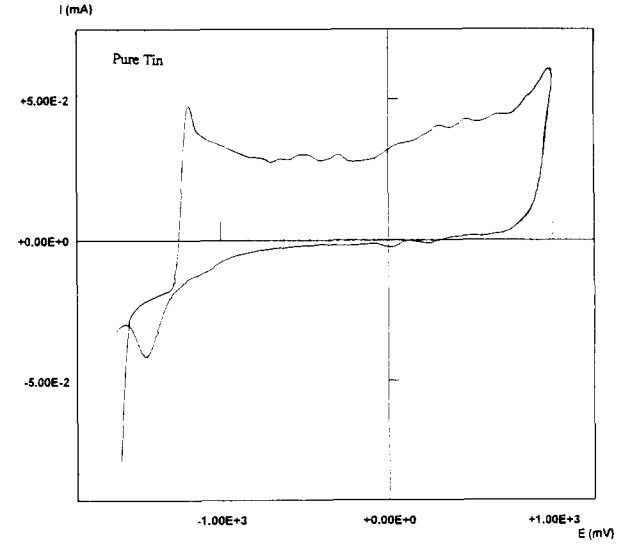

Fig. 2. Cyclic voltammogram for pure tin in 0.1 M $Na_2B_4O_7$. Scan rate: 10 mV s^{-1}.

increasing alloying tin content, the shoulder becomes more and more defined. Peak C_2 is likely to be associated with the formation of α-PbO_2, the only stable oxide that can form in alkaline solution [11]. Here again, the inhibition of the formation of PbO_2 by alloying with tin is to be noted. It is possible that a high valency mixed lead–tin oxide is produced, as suggested by Pavlov et al. [12] and Bojinov et al. [13]. Peak C_1 can be related to the formation of PbO_x ($1 < x \leqslant 1.5$) [9,12–14] through various lead oxidation states, for example +2.67 (Pb_3O_4), +3 (Pb_2O_3), with a large overpotential due to a decrease of the surface pH that results from the release of protons in the anodic reactions.

During the reverse scan of the voltammogram, two small cathodic peaks D1 and D2 can be observed (Fig. 1). These peaks are thought to correspond, respectively, to the partial reductions of PbO_2 into PbO_x and PbO_x into PbO. PbO_x could be Pb_3O_4, since the redox potentials of PbO_2/Pb_3O_4 and Pb_3O_4/PbO are, respectively, +54 and −215 mV, i.e., values that are not far from the potentials of peaks D1 and D2. The non-conducting property of the PbO layer is thought to be responsible for the slowing down of the reduction rate. The cathodic peak (E) on pure lead is assumed to come from the reduction of the residual PbO, PbO_x and PbO_2. It can be seen that peak (E) decreases as the tin level in the alloys increases. This behaviour supports the suggestion that tin inhibits the formation of PbO and PbO_2. As the tin level increases, peak E_2 becomes more defined. This peak may be related to the reduction of residual PbO_x.

Peak E_3 is obviously connected to the reduction of SnO_2 to Sn, as can be seen on the voltammogram for pure tin (Fig. 2). It was observed that the passive current density, at any potential, decreased as polarization time was increased. So, in order to evaluate the effect of alloying tin on the passive current density, each alloy was prepolarized for 5 min at −2500 mV then polarized at 0 mV (i.e., in the middle of the passivity range) for a time that was sufficient to attain a steady-state current. The steady-state passive current density (I_p) decreased when the tin content in lead alloys increased. This property is illustrated in Fig. 3.

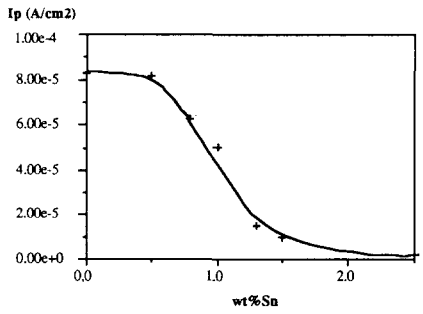

Fig. 3. Variation of passivation current (I_p) measured by potentiostatic polarization at 0 V, in deaerated 0.1 M $Na_2B_4O_7$.

In terms of the corrosion resistance, the value of the current density is usually related to the stability of the passive layer. The steady-state, passive current density, according to Vetter [15], represents the dissolution rate. The latter is equal to the formation rate of the passive layer. So, for a passive layer to be stable and protective, it must have a very low dissolution rate. For pure lead and lead–tin alloys, high I_p means high dissolution rate or high ionic activity of the oxide layer, in this case PbO. Above 1.5 wt.% Sn, I_p tends to be very low, namely, $\sim 10^{-6}$ A cm^{-2}. In this work, the I_p of pure tin, as measured under the same conditions as lead–tin alloys, was 3.5×10^{-7} A cm^{-2}. So, the higher the tin content, the higher the corrosion resistance of the alloys in 0.1 M $Na_2B_4O_7$ solution.

3.2. Polarization of ferro/ferricyanide couple in 0.1 M $Na_2B_4O_7$

Polarization curves are given in Fig. 4. Even in the presence of the redox system, no additional current was observed for pure lead, or for 0.5 and 0.8 wt.% Sn alloys. This means that no transfer of electrons has taken place through the passive layer and, therefore, the oxidation of ferrocyanide or the reduction of ferricyanide is prevented. On the other hand, 1, 1.3, 1.5, and 2.5 wt.% lead–tin alloys allow the redox reactions of ferri/ferrocyanide to take place on their passive films. The currents measured were the sum of the passive currents of the alloys and the polarization currents of the redox couple. The higher the alloying tin level, the higher the kinetics of the redox reaction. From this result, it can be concluded that the passive films formed on alloys having a tin content higher than 1 wt.% present an electronic conductivity, while the low-tin alloy films present an approximate ionic conductivity.

The total current densities in absolute values (Fig. 4) are considered to be $I_a = I_a(\text{redox}) + I_p$ and $I_c = I_c(\text{redox}) - I_p$. Polarization current densities of the redox reaction alone, $I_a(\text{redox})$ and $I_c(\text{redox})$, have been calculated from these relations and are plotted in Fig. 5. It can be seen that the effect of alloying tin is to

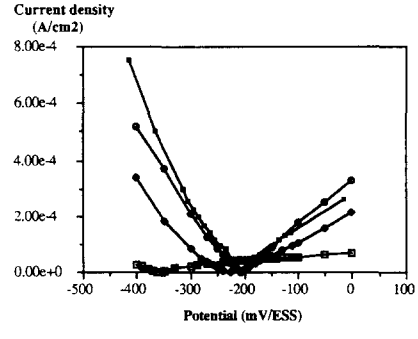

Fig. 4. Polarization curves of alloys in deaerated 0.1 M tetraborate solution containing 0.025 M ferri/ferrocyanide. □, 1 wt.% Sn; ◆, 1.3 wt.% Sn; ●, 1.5 wt.% Sn; ■, 2.5 wt.% Sn.

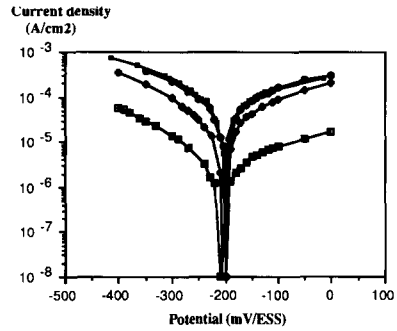

Fig. 5. Polarization curves of ferri/ferrocyanide redox couple (0.025 M) on lead–tin alloys in deaerated 0.1 M $Na_2B_4O_7$, □, 1 wt.% Sn; ♦, 1.3 wt.% Sn; ●, 1.5 wt.% Sn; ■, 2.5 wt.% Sn.

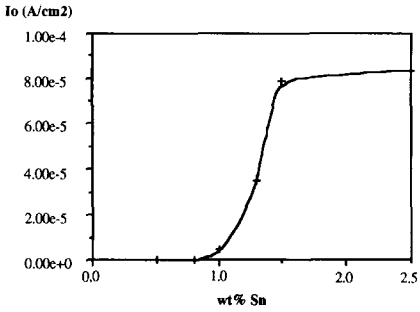

Fig. 6. Variation of exchange-current density, I_0, of ferri/ferrocyanide redox couple vs. tin content in deaerated 0.1 M $Na_2B_4O_7$.

increase the redox reaction rate, that is to facilitate electronic exchange at the alloy/solution interface. The tin content of the alloy must be higher than 1.5 wt.% to infer good electronic conductivity through the passive film. The redox kinetics decrease with lower tin contents (as can be seen for 1.3 and 1 wt.% alloys) and then become negligible for 0.8, 0.5 wt.% Sn and pure lead.

The values of the polarization currents and the applied potential for the redox reactions (Fig. 4) have been used to calculate, by a 'Simplex' computing program [16,17], the exchange current density. Fig. 6 shows the relation between the exchange-current density and the tin content of the alloy. The exchange-current density, I_0, is insignificant for alloy with less than 0.8 wt.% Sn. When the tin content is increased from 1 to 1.5 wt.%, I_0 increases sharply and attains a plateau for alloys with 1.5–2.5 wt.% Sn. The change in I_0 illustrates the change in the conductivity of the film, from an ionic to an electronic type. The electronic conductivity of the passive film is assumed to be induced by the presence of SnO_2 that results from the oxidation of the alloying tin. Surface analyses, mainly by XPS, are then necessary to determine the amount of SnO_2 in the passive PbO film, and to elucidate the mechanism of the role played by tin.

3.3. XPS qualitative analysis of passive layers

Fig. 7 shows the spectra of Sn level $3d_{5/2}$ and Sn level $3d_{3/2}$ in the passive films of lead tin–alloys. Peaks

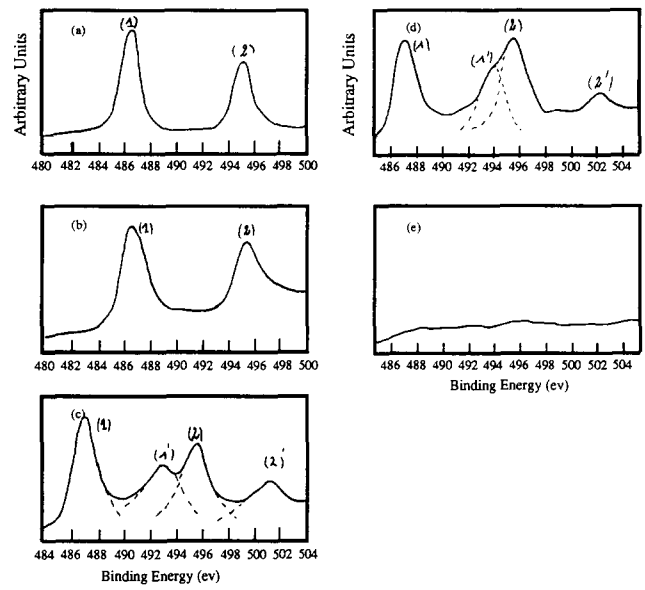

Fig. 7. Spectra of tin ($3d_{5/2}$ (2) and $3d_{3/2}$ (1)) in passive films on lead–tin alloys, after 3 min sputtering.

1 and 2 in Fig. 7(a) and (b) of the 2.5 and 1.5 wt.% Sn alloys are associated with oxidized tin [18]. The signals of SnO and SnO_2 have been found to be very close [19,20], so it is not possible to determine whether SnO and SnO_2 are present in the passive film. The spectra of alloys with lower tin contents display two other peaks, denoted as 1′ and 2′ (Fig. 7(c), (d)). The binding energies that correspond to the tin spectra of the alloys are gathered in Table 1. It can be seen that the difference between the two 3d energy levels of oxidized tin (peak 2 − peak 1) is 8.5 eV and the difference peak 2′ − peak 1′ is roughly 8.4 eV. It is then likely that peaks 1′ and 2′ are shifted from peaks 1 and 2 and are related to oxidized tin signals. The shifting of the binding energy to higher levels may have two origins. The first is a change in the oxidation state or the chemical environment of the element, that leads to stronger electronic binding. The second is a decrease in the electrical conductivity of the sample: the emission of electrons following X-ray irradiation will result in the appearance of positive charges on the surface of the sample. If the sample (the passive layer, in this case) is an insulator or has a very low conductivity, the non-neutralized positive charges will increase the binding energy of electrons in the surface ions and the XPS peaks will shift to higher energy levels. The parameters reported in Table 1 show that the shifting of oxidized tin signals 1 and 2 to 1′ and 2′ is roughly 5.6 eV (peak 1 − peak 1′ or peak 2 − peak 2′) for 1.3 wt.% Sn alloy and 6.6 eV for 1 wt.% Sn alloy. These are quite high values compared with the shift of the binding energy due to the increase of the oxidation state or to the bonding of tin with a strongly electronegative element, such as in SnF_4. In fact, it is reported

Table 1
Binding energy (eV) of tin spectra for lead–tin alloys

Alloy (wt.% Sn)	Sn(ox) $3d_{3/2}$ (peak 2)	Sn(ox) $3d_{5/2}$ (peak 1)	Peak 2′	Peak 1′	Peak 2 − peak 1	Peak 2′ − peak 1′
2.5	495.0	486.5			8.5	
1.5	495.2	486.7			8.5	
1.3	495.6	487.1	501.1	492.7	8.5	8.4
1	495.6	487.1	502.1	493.7	8.5	8.4
0.5						
Tin oxide [17]	494.9	486.4			8.5	

that the shift of the tin signals, when tin is oxidized from SnO to SnO_2, is not significant [19,20], and that the shift from SnO to SnF_4 is only 1.2 eV [20]. Therefore, it can be stated that for alloys with less than 1.5 wt.% Sn, the passive layers include positively charged zones because of low electrical conductivity. As the tin content decreases, so does the electrical conductivity of the passive layer [21], and the XPS signals undergo a greater shift (Table 1).

The existence of two types of signals, the shifted and the unshifted, can be explained by the presence of both charged and uncharged zones. When the tin content is higher than 1.5 wt.%, only the uncharged zones are assumed to be present in the passive layer (Fig. 7(a), (b)). This characteristic should be related to the conductivity study that showed these passivated alloys to have a high electronic conductivity in a redox solution. On the other hand, the same in situ study revealed that the conductivity of the passive layers decreased sharply when the alloying tin was decreased from 1.3 to 1 wt.%, to become negligible for 0.5 wt.% Sn. This behaviour is now verified by XPS results that demonstrate the shifting of signals, due probably to the non-conducting property of the corresponding passive layers. For 0.5 wt.% Sn alloy, no signal of oxidized tin was observed. This means that the non-conducting passive films contained no tin oxide, at least in the outer layer.

3.4. XPS quantitative analysis of passive films

Semi-quantitative analysis of passive layers was made by the XPS equipment used in this study. The computer programme comprised an iterative calculation method based on a χ^2 criterion that allows quantification of elements according to experimental intensities.

Semi-quantitative analysis of the passive films followed each sputtering time. The latter varied from 3 to 30 min. Longer sputtering was not employed because of possible disturbances that could increase the uncertainty of the results (e.g., increase of surface temperature, change in the nature of the bonds). The results are reported in Fig. 8. The concentration of tin (calculated as wt.%) changed sharply during the first 3 min of sputtering. It is assumed that the contamination layer was removed after this first ion-scraping. For conducting passive films on 2.5 and 1.5 wt.% Sn alloys, it is noted that the concentration of tin is markedly increased by an average of 42 and 27%, respectively. Enrichment of tin in the passive layer was also observed for low and non-conducting alloys. For 1.3 and 1 wt.% Sn alloys, the tin content increased continuously up to 15 wt.% in the inner layer at a sputtering time of 30 min. It was nearly 3 wt.% in the inner layer of non-conducting 0.5 wt.% Sn alloy.

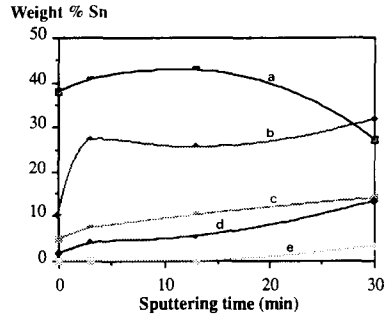

Fig. 8. Depth profile of tin in passive layers of lead–tin alloys. a, 2.5; b, 1.5; c, 1.3; d, 1.0; e, 0.5 wt.% Sn.

The reason for a fast decrease of tin content in the passive film of 2.5 wt.% Sn alloy (from 42 to 27 wt.% between 13 and 30 min sputtering time) may come from the thinness of the passive layer under the effect of tin [22,23] and the increase of the intensity of the signal for metallic lead. To explain the particular enrichment of tin in the passive film, it is necessary to consider the solubility of the species involved in the process of the film formation. As the film is formed by the polarization of lead–tin alloys at 0 V in alkaline solution (pH = 9.1), Pb is oxidized to $Pb(OH)_2$ in the first step [21]. The solubility of this hydroxide is 155 mg per litre of cold water [24]. Meanwhile, tin is oxidized probably to SnO, then oxidized again to SnO_2, the only thermodynamically stable compound of tin under these conditions of pH and potential. SnO_2 is sparingly soluble [24]. Therefore, in the passive layer, there is first a selective dissolution of lead as soluble lead hydroxide, and later, sparingly soluble PbO is formed. Part of the PbO might react with transitory SnO to give Pb and SnO_2. By this dismutation reaction,

the PbO layer becomes thinner and the enrichment of tin, as SnO_2, becomes higher, when sufficient alloying tin is present, such as in 2.5 and 1.5 wt.% Sn alloys.

The conductivity of the passive layers, as evaluated by the previous in situ study, can now be related to the particularly high content of conducting SnO_2. In non-conducting passive layers (0.5 wt.% Sn alloy), the concentration of tin in the inner layer is found to be 3 wt.% (Fig. 8). One of the proposed mechanisms of the action of tin on the electrical property of PbO has been the doping of PbO by tin [12,14,25]. But, doping usually requires only small amounts of dopant. This study shows that the increase in the conductivity of the passive layer demands a concentration of tin that is higher than 10 wt.%!

3.5. Electrochemical impedance spectroscopy of lead–tin alloys in 0.1 M $Na_2B_4O_7$

Pure lead, pure tin and lead–tin alloys were polarized in 0.1 M $Na_2B_4O_7$ solution at 0 V, i.e., in the passivity domain. Impedance measurements were performed after a constant current was obtained, that is between 15 and 24 h (depending on the alloy composition).

Fig. 9 shows the Nyquist plot obtained for the different lead–tin alloys, pure tin and pure lead. For pure tin and the various lead–tin alloys, diffusion control is observed at low frequencies. For pure lead, the complex plane plot follows a semicircle that can be described, in a first approach, by an equivalent circuit made up of a polarization resistance, R_p, in parallel with a double-layer capacitance, C_{dl}. For lead–tin alloys, a Warburg-type impedance must be considered and added in series with R_p. The diffusion control appears to be associated with the presence of tin oxide in the corrosion layers.

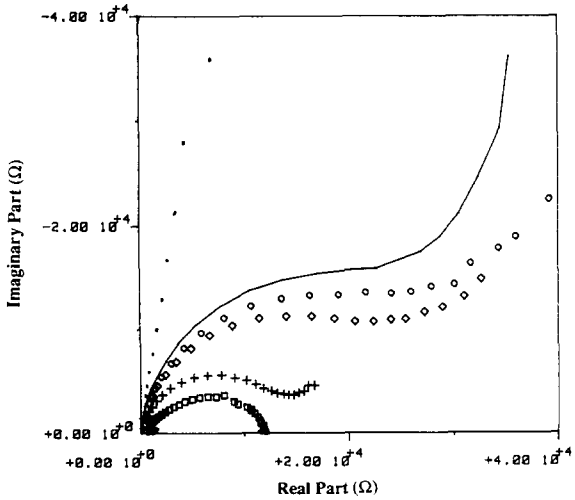

Fig. 9. Nyquist plots for pure tin, pure lead and different lead–tin alloys, after polarization in 0.1 M $Na_2B_4O_7$ at 0 V. □, Pure lead; +, 1 wt.% Sn; ◇, 1.3 wt.% Sn; ○, 1.5 wt.% Sn; —, 2.5 wt.% Sn; ●, pure tin.

The polarization resistance, R_p, obtained by extrapolating the semicircle toward zero frequency, increases when the alloying tin content is increased. For pure tin, the sharp increase in impedance indicates that the electrode is passivated by an SnO_2 layer [21], which behaves as an ionic non-conductor. The dependence of the values of R_p versus the tin content in the alloys is in good agreement with the previous electrochemical study.

A Bode plot of the impedance is represented in Fig. 10(a) and (b). This shows the dependence of the modulus and the phase, respectively, versus frequency. At high frequencies, the modulus for the different lead–tin alloys and pure tin appear to be independent of the frequency, except for pure lead, and approach a constant value of the electrolytic resistance R_e. The modulus of pure lead is, however, one order of magnitude higher than for the other lead–tin alloys studied. In the in situ

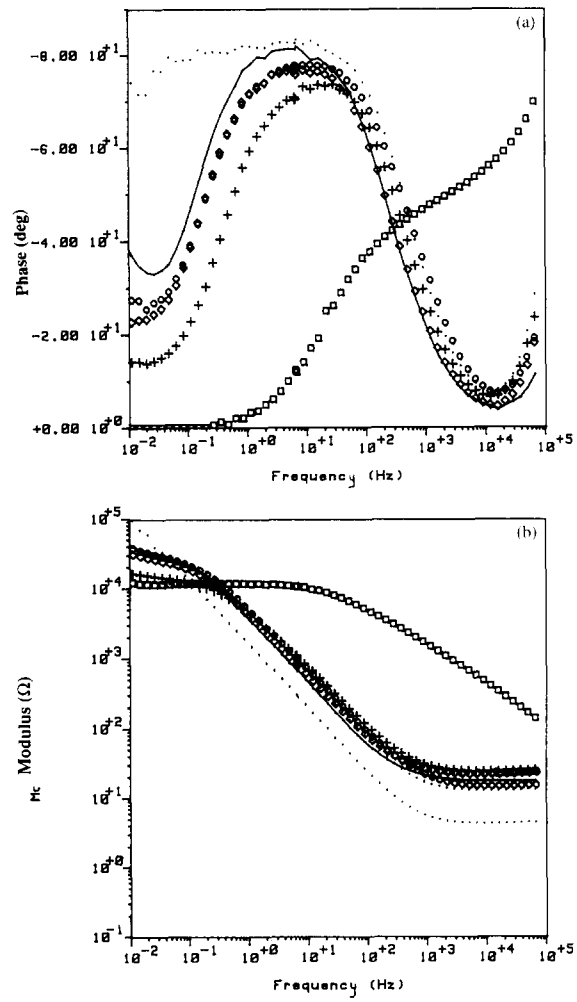

Fig. 10. Bode plots for pure tin, pure lead and different lead–tin alloys, after polarization in 0.1 M $Na_2B_4O_7$ at 0 V: (a) modulus vs. frequency plot; (b) phase vs. frequency plot. □, Pure lead; +, 1 wt.% Sn; ◇, 1.3 wt.% Sn; ○, 1.5 wt.% Sn; —, 2.5 wt.% Sn; ●, pure tin.

Table 2
Best-fit values for equivalent circuit for pure-lead electrode in 0.1 M $Na_2B_4O_7$

C_{sc} (F)	R_{ss} (Ω)	C_{ss} (F)	R_{ct} (Ω)	C_{dl} (F)	CPE 1	CPE 2	R_e (Ω)	Fitting corr.
310^{-8}	220	1.5×10^{-9}	10300	2.6×10^{-6}	0.63	0.65	220	0.9996

conductivity study, it has been shown that passive layers formed on lead–tin alloys with a tin content higher than 0.8 wt.% exhibit good electronic conductivity while the passive layer formed on pure lead is more resistive. The high values of the modulus at high frequency for pure lead confirm the previous results in the sense that alloying with tin improves the electronic conduction of the passive layers. At low frequencies, however, it can be seen that the impedance modulus of pure lead is lower than for tin alloys. This behaviour indicates that the polarization resistance of tin alloys is higher than that for pure lead, in agreement with their higher corrosion resistance found previously.

The phase versus frequency plots (Fig. 10(b)) reveal a marked difference in the impedance characteristics of tin alloys. At high frequencies, the high value of the phase angle of lead may be explained by the semiconducting properties of the PbO layer [26]. To interpret this impedance behaviour of lead, the equivalent circuit generally used for semiconductors was applied [27] with the addition of a constant phase element (CPE), to account for the frequency dispersion, and a parallel capacitance C_{dl} at the PbO/electrolyte interface (Fig. 11). The best-fit values of the equivalent circuit using the 'Simplex' fitting procedure are listed in Table 2. An example of the calculated phase and modulus versus frequency plots is shown in Fig. 12.

For tin-rich alloys, the surface film is composed of mixed or composite lead–tin oxide, which is electronically conducting. The impedance can be described by a simpler equivalent circuit (Fig. 13) where a Warburg-type impedance $Z\omega$ is added to account for the ionic diffusion through the surface film. The best-fit parameters are listed in Table 3. An example of the calculated phase and modulus versus frequency plots is shown in Fig. 14.

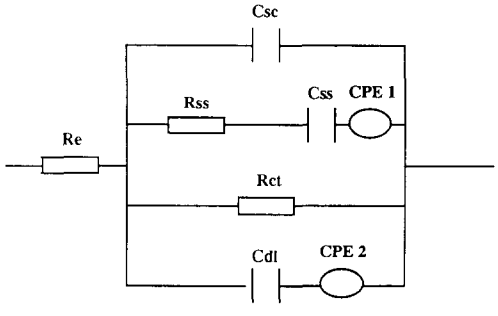

Fig. 11. Proposed equivalent circuit for pure-lead electrode in 0.1 M $Na_2B_4O_7$. R_e = resistance of electrolyte; C_{sc} = space charge capacitance; R_{ss} = surface states resistance; C_{ss} = capacitance relative to storage of charge on surface states; R_{ct} = charge-transfer resistance; C_{dl} = double-layer capacitance; CPE = constant phase element.

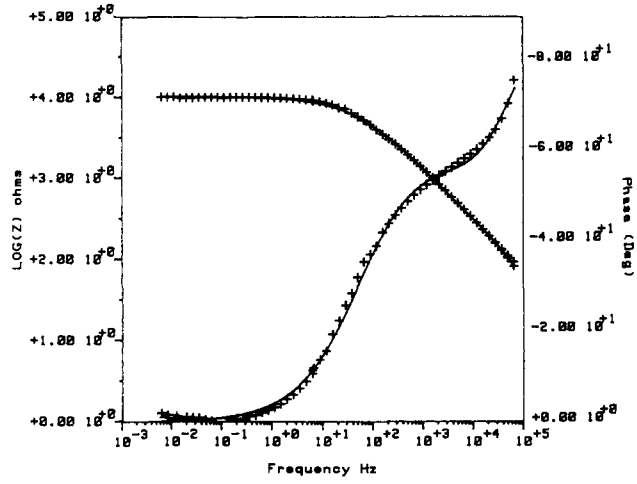

Fig. 12. Calculated (—) and experimental (+ +) phase and modulus vs. frequency plots for pure lead in 0.1 M $Na_2B_4O_7$, using equivalent circuit shown in Fig. 11.

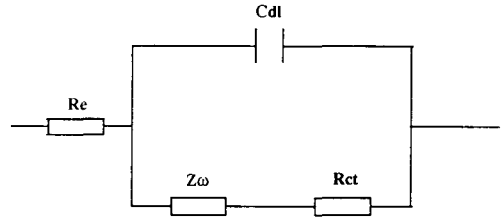

Fig. 13. Proposed equivalent circuit for lead–tin alloys, after polarization in 0.1 M $Na_2B_4O_7$.

Table 3
Best-fit values for equivalent circuit for lead–tin alloy electrodes in 0.1 M $Na_2B_4O_7$

Alloy (wt.% Sn)	C_1 (F)	R_1 (Ω)	R_e (Ω)	CPE	Fitting corr.
1	7.4×10^{-6}	13000	23	0.86	0.9998
1.3	1.2×10^{-6}	23600	22	0.88	0.9998
1.5	10×10^{-6}	27200	16	0.88	0.9997
2.5	20×10^{-6}	28600	18	0.92	0.9996

The electrochemical impedance behaviour may then be interpreted by the high polarization resistance and the high capacitance of the tin-rich alloys, the passive layers of which are enriched with corrosion-resistant SnO_2, as shown earlier. In other words, SnO_2 may be considered as a barrier for ionic conduction through the passive film that increases the electrochemical

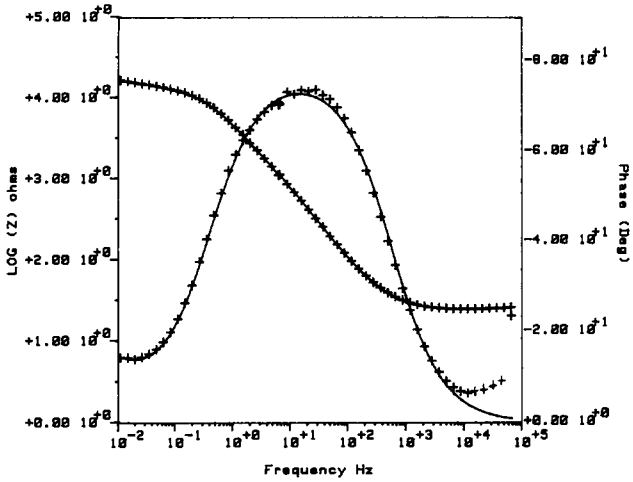

Fig. 14. Calculated (——) and experimental (+ +) phase and modulus vs. frequency plots for 1 wt.% Sn in 0.1 M $Na_2B_4O_7$, using equivalent circuit shown in Fig. 13.

impedance. This, in turn, translates the resistance to ionic exchange at the electrode/electrolyte interface, at low frequencies.

This electrochemical impedance spectroscopic study of the alloy/passive-layer electrode in solution at pH = 9.1 confirms previous results obtained by electrochemical and XPS analyses, and shows that the role of tin, under the form of SnO_2, consists of changing the semiconducting properties of the PbO layer which becomes more electronically conductive.

3.6. Electrochemical impedance spectroscopy of lead–tin alloys in 1 M H_2SO_4

Lead–tin alloys and pure lead were polarized in 1 M H_2SO_4 solution. The potential scan was commenced at −1500 mV at a rate of 1 mV s^{-1}. The electrodes were then held at +400 mV for 40 h. Under these conditions, the pure-lead electrode can be described as a $Pb/PbO/PbSO_4$ duplex system. A steady state-passive current was obtained, and the electrochemical impedance spectroscopic measurements were then performed. Fig. 15 represents the Nyquist plots for the lead–tin alloys and pure lead. The variation of the cell impedance with frequency follows a semicircle for both pure lead and lead–tin alloys. It appears that control by diffusion of charged species is absent. The polarization resistance, determined from the intercept of the semicircle with the real part of the cell impedance at low frequencies, decreases when the tin content of the alloys decreases. These results are different from those obtained in solution at pH = 9.1 where ionic diffusion control is clearly observed and it is found that tin has the property of increasing the corrosion resistance of the alloys. The data in Fig. 15, however, show that the corrosion resistance of the alloys in 1 M H_2SO_4 decreases, i.e., the dissolution rate of the alloys increases,

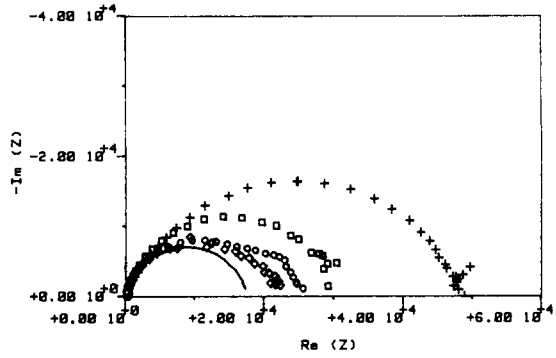

Fig. 15. Nyquist plots for pure lead and different lead–tin alloys, after 40 h polarization in 1 M H_2SO_4 at +400 mV. +, pure lead; □, 1 wt.% Sn; ◇, 1.3 wt.% Sn; ○, 1.5 wt.% Sn; ——, 2.5 wt.% Sn.

when the tin content increases. This behaviour can be explained by the facility of tin to dissolve in sulfuric acid through the passive layer, as shown by the ring-disc measurements of Bojinov et al. [13]. As the corrosion rate is purely activation-controlled, the polarization resistance for pure lead is the highest because of the presence of the passive PbO layer underneath the sulfate layer. This PbO layer has been shown [21] to become thinner and more electronically conductive when the tin level in the alloy is increased. This property may explain the decrease in the activation energy that controls the dissolution kinetics of the alloys. In other words, the decrease of the polarization resistance is connected to the increase of the tin content. These impedance results may find confirmation in the works of several authors [9.28], who observed an increase in the passive current density measured in the potential range of the PbO formation in H_2SO_4.

The modulus and the phase angle versus frequency plots of the cell impedance are presented in Fig. 16. The modulus obtained for pure lead is one order of magnitude higher, at high frequencies, than that for lead–tin alloys. As the effect of the solution and film resistance can only be seen at high frequencies, it can be stated that the passive layers formed on lead–tin alloys are much more conductive than that formed on pure lead. The PbO layer beneath the sulfate layer has been shown to have semiconducting properties [12,25,26]. The duplex structure $PbO/PbSO_4$ of the passive film formed on pure lead can be described by the previous equivalent circuit used for semiconductors in which the capacitance C_{dl} is now related to the sulfate/electrolyte interface. The best-fit parameters are listed in Table 4. An example of the calculated phase and modulus versus frequency plots is given in Fig. 17.

For tin alloys, the inner layer is highly conductive due to the presence of tin. The simulation of the experimental results can now be performed with a simpler equivalent circuit that is composed of a parallel combination of R_{ct} and C_{dl} representing the sulfate layer, in series with another parallel R_1–C_1 combination,

Table 4
Best-fit values for equivalent circuit for pure-lead electrode in 1 M H_2SO_4

C_{sc} (F)	R_{ss} (Ω)	C_{ss} (F)	R_{ct} (Ω)	C_{dl} (F)	CPE 1	CPE 2	R_e (Ω)	Fitting corr.
5×10^{-8}	190	2×10^{-9}	51300	2×10^{-6}	0.68	0.88	0.2	0.9999

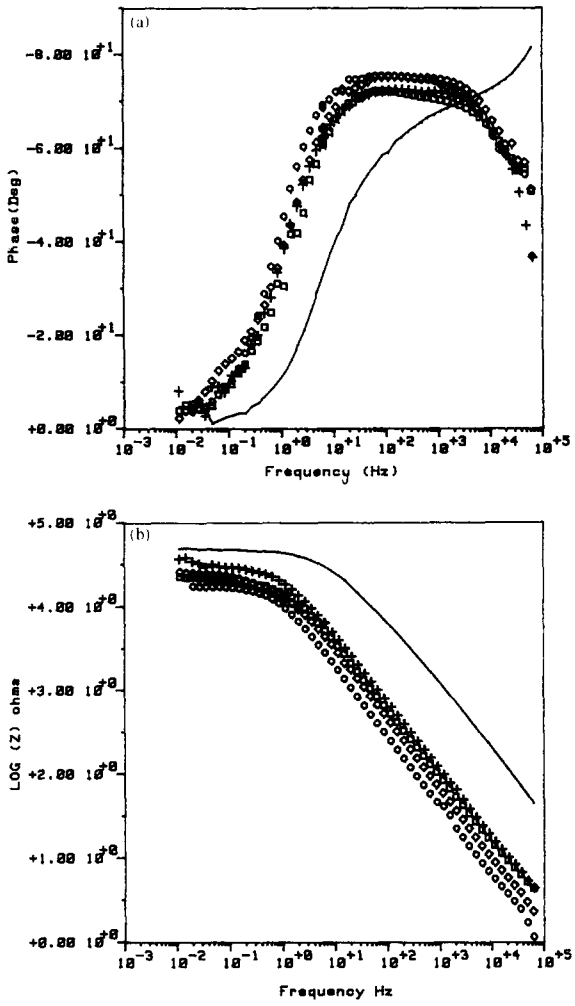

Fig. 16. Bode plots for pure lead and different lead–tin alloys, after 40 h of polarization in 1 M H_2SO_4 at +400 mV: (a) modulus vs. frequency plot; (b) phase vs. frequency plot. +, pure lead; □, 1 wt.% Sn; ◇, 1.3 wt.% Sn; ○, 1.5 wt.% Sn; —, 2.5 wt.% Sn.

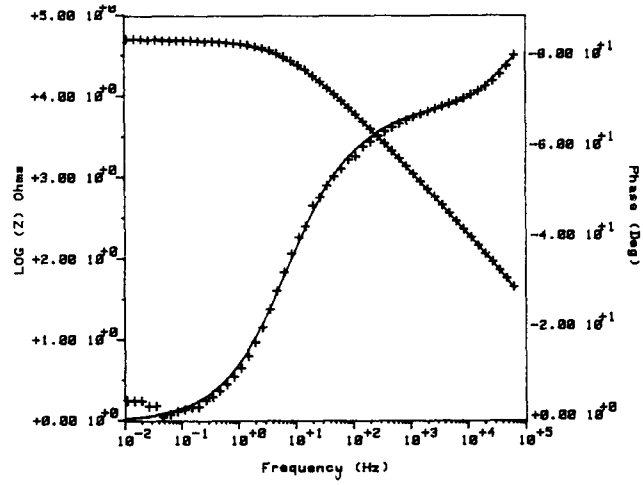

Fig. 17. Calculated (—) and experimental (+ +) phase and modulus vs. frequency plots for pure lead in 1 M H_2SO_4, using equivalent circuit shown in Fig. 11.

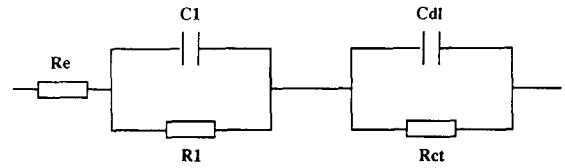

Fig. 18. Proposed equivalent circuit for lead–tin alloys in 1 M H_2SO_4. R_{ct} = charge transfer at $PbSO_4/H_2SO_4$ interface; C_{dl} = capacitance of $PbSO_4/H_2SO_4$ interface; R_1 = resistance of inner layer; C_1 = capacitance of inner layer; R_e = resistance of electrolyte.

to take account of the conducting inner layer (Fig. 18). The data listed in Table 5 show that R_1 is quite small, and the contribution of this layer to the electrode impedance is negligible. An example of the calculated phase and modulus versus frequency plots is given in Fig. 19.

The frequency dependence of the phase angle of pure lead at high frequencies exhibits the same features in both 1 M H_2SO_4 and 0.1 M $Na_2B_4O_7$. At high frequencies up to 10^5 Hz, however, the high values of the phase angle of pure lead cannot be explained by the values of the polarization resistance which are higher than those of tin alloys, but may be interpreted by the presence of a semiconducting PbO layer beneath the $PbSO_4$ layer, and a low value of the capacitance due to the thickness of the layer.

At low frequencies, the phase angles of the different electrodes tend to zero. This means that no diffusion-control occurred, unlike in the previous observations in 0.1 M $Na_2B_4O_7$. To explain these features, it is reasonable to state that passivation did not occur in sulfuric acid solution, for it is known that tin dissolves in this medium [13]. Even with the increase of pH, due to OH^- diffusion through the sulfate layer, the presence of SO_4^{2-} and adsorbed tin ions in the PbO layer could induce more ionic conduction. This is the reason why the observed polarization resistance decreases when the tin content in the alloys is increased. This explanation is in agreement with the work of Pavlov et al. [12] who state that the PbO layer is no longer passive when tin ions, in the Sn^{2+}, Sn^{3+} or Sn^{4+} state, are adsorbed in the layer.

The same study has been carried out in 5 M H_2SO_4. The electrochemical impedance spectra obtained after

Table 5
Best-fit values for equivalent circuit for lead–tin alloy electrodes in 1 M H_2SO_4

Alloy (wt.% Sn)	R_e (Ω)	R_t (Ω)	C_1 (F)	R_{ct} (Ω)	C_{dl} (F)	CPE 1	CPE 2	Fitting corr.
1	0.2	2.1	1×10^{-7}	30600	5×10^{-7}	0.73	0.80	0.9997
1.3	0.2	2.7	3×10^{-7}	20700	6×10^{-7}	0.66	0.81	0.9998
1.5	0.3	1.5	6×10^{-7}	20800	1.2×10^{-6}	0.71	0.84	0.9999
2.5	0.2	1.5	1.2×10^{-6}	17500	2.3×10^{-6}	0.75	0.85	0.9999

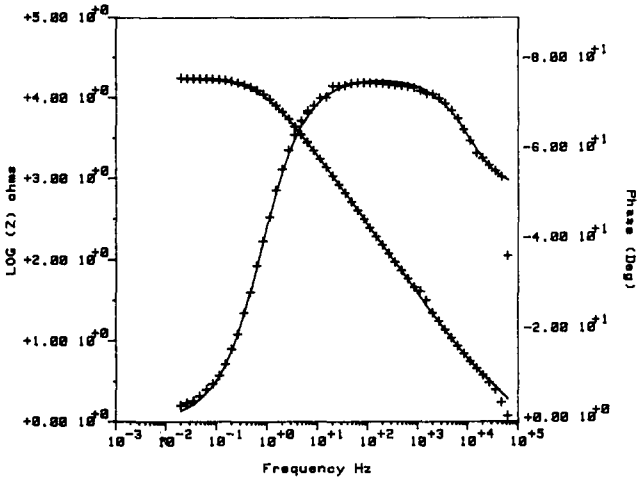

Fig. 19. Calculated (—) and experimental (+ +) phase and modulus vs. frequency plots for 2.5 wt.% Sn in 1 M H_2SO_4, using equivalent circuit shown in Fig. 18.

40 h of polarization at 400 mV present the same features as in 1 M H_2SO_4, with the same effect of alloying with tin on the polarization resistance, the modulus and the phase angle of the electrode impedance. Change in acid concentration does not lead to a difference in the behaviour of the alloys under the passivation treatment.

4. Conclusions

This study of the effect of alloying tin on the passive layers formed on lead–tin alloys in two different media, namely, 0.1 M $Na_2B_4O_7$ (pH=9.1) and 1 M H_2SO_4, has led to the following conclusions.

(1) Passive films on low-tin alloys (<0.8 wt.% Sn) have no electronic conductivity, only ionic conductivity.

(2) The electronic conductivity of the passive films increases sharply when the alloying tin content increases from 1 to 1.5 wt.% Sn, and attains a plateau between 1.5 and 2.5 wt.% Sn.

(3) Passive current densities decrease, or the corrosion resistance of lead–tin alloys increases, with increasing tin content in the alloy.

(4) A minimal tin content of ~1.5 wt.% is required to ensure a high electronic conductivity of the passive films (in pH=9) and a high resistance to corrosion.

(5) XPS signals for tin, lead and oxygen (the main components of passive films) are depleted in unshifted and shifted signals when the conductivity of the passive films (evaluated by electrochemical study) becomes very low.

(6) The shifted signals are assumed to have originated from positively charged zones on the surface film due to the low conductivity. The degree of shifting increases when the alloying tin content is decreased, i.e., when the film conductivity is decreased.

(7) The concentration of tin (as compared with lead) in the passive films is largely increased, up to 44, 28, 14, 13 and 3 wt.%, respectively, for 2.5, 1.5, 1.3, 1 and 0.5 wt.% Sn alloys.

(8) Semi-quantitative analysis shows that one of the effects of tin could be the thinning of the passive films, as observed for 2.5 wt.% Sn alloy. The inner layer of the passive films is found to be rich in conducting tin oxide and metallic lead.

(9) Alloying tin has the effect of inhibiting the oxidation of lead to PbO and PbO_2 in 0.1 M $Na_2B_4O_7$, but does not appear to hinder the formation of an intermediate compound, PbO_x.

(10) The polarization resistance of passivated electrodes increases in 0.1 M $Na_2B_4O_7$ when the tin content increases, but the resistance decreases in sulfuric acid solution.

(11) The electrochemical behaviour of lead and lead–tin alloys can be described fully by an equivalent circuit. This comprises a combination of elements that represent a semiconducting electrode for pure lead. The simulation shows that tin has an effect of transforming the semiconducting lead oxide layer into a highly conductive layer.

(12) Tin oxide is stable in solutions of pH=9.1. It increases the electronic conductivity and decreases the ionic conductivity of the mixed lead–tin oxide. On the other hand, tin oxide is unstable in sulfuric acid and increases the ionic conductivity of the passive layer.

References

[1] J. Burbank, *J. Electrochem. Soc., 106* (1959) 369.
[2] J. Lander, *J. Electrochem. Soc., 98* (1951) 213.

[3] D. Pavlov, C.N. Poulieff, E. Klaja and N. Iordanov, *J. Electrochem. Soc., 116* (1969) 316.
[4] P. Rüetschi, *J. Electrochem. Soc., 120* (1973) 331.
[5] J.S. Buchanan, N.P. Freestone and L.M. Peter, *J. Electroanal. Chem., 182* (1985) 383.
[6] J.S. Buchanan and L.M. Peter, *Electrochim. Acta, 33* (1988) 127.
[7] K. Takashi, N. Hoshihara, H. Yashuda, T. Ishii and H. Jinbo, *J. Power Sources, 30* (1990) 23.
[8] B. Culpin, A.F. Hollekamp and D.A.J. Rand, *J. Power Sources, 38* (1992) 63–74.
[9] R.F. Nelson and D.M. Wisdom, *J. Power Sources, 33* (1991) 165.
[10] M.T. Shevalier and V.I. Birss, *J. Electrochem. Soc., 137* (1990) 2643.
[11] M. Pourbaix, *Atlas d'Equilibres Electrochimiques à 25 °C,* Gauthier-Villars, Paris, 1963, p. 485.
[12] D. Pavlov, B. Monhakov, M. Maja and N. Penazi, *J. Electrochem. Soc., 136* (1989) 27.
[13] M. Bojinov, K. Salmi and G. Sundholm, *Electrochim. Acta, 39* (1994) 719.
[14] H. Doëring, J. Garche, H. Dietz and K. Wiezener, *J. Power Sources, 30* (1990) 41.
[15] K.J. Vetter, *Z. Elektrochem., 62* (1958) 642.
[16] J.A. Nelder and R. Mead, *Comput J., 7* (1965) 308.
[17] P.B. Ryan, R.L. Barr and H.D. Todd, *Anal. Chem., 52* (1980) 1460.
[18] A.W.C. Lin, R.N. Armstrong and T. Kwana, *Anal. Chem., 49* (1977) 1228.
[19] C.D. Wagner, W.M. Riggs, L.E. Davis and J.F. Marlder, in G.E. Muilenberg (ed.), *Handbook of X-Ray Photoelectron Spectroscopy,* Perkin-Elmer Corporation, 1979.
[20] P.A. Gutsch, M.V. Zeller and T.P. Fehlner, *Inorg. Chem., 12* (1973) 1432.
[21] P. Simon, N. Bui and F. Dabosi, *J. Power Sources, 50* (1994) 141.
[22] R.T. Barton, P.J. Mitchell and F.A. Fleming, in T. Keily and B.W. Baxter (eds.), *Power Sources 13, Research and Development in Non-Mechanical Electrical Power Sources,* International Power Sources Committee, Leatherhead, UK, 1991, p. 25.
[23] H.K. Giess, in K.P. Bullock and D. Pavlov (eds.), *Proc. Symp. Advances in Lead–Acid Batteries,* Proc. Vol. 84-14, The Electrochemical Society, Inc. Pennington, NJ, USA, 1984, p. 241.
[24] R.C. Weast (ed.), *Handbook of Chemistry and Physics,* CRC, Boca Raton, FL, 66th edn., 1985–1986.
[25] J. Garche, *J. Power Sources, 30* (1990) 47.
[26] F.E. Varela, L.M. Gassa and J.L. Vilche, *J. Electroanal. Chem., 353* (1993) 147.
[27] S.R. Morisson, *Electrochemistry of Semiconductor and Oxidized Electrodes,* Plenum, New York, 1984.
[28] M.N.C. Ijomah, *J. Appl. Electrochem., 18* (1988) 142.